Bioorganic & Medicinal Chemistry Letters 21 (2011) 1795–1801

Contents lists available at ScienceDirect

Bioorganic & Medicinal Chemistry Letters

journal homepage: www.elsevier.com/locate/bmcl

Design and synthesis of novel allosteric MEK inhibitor CH4987655 as an orally available anticancer agent

Yoshiaki Isshiki [a,*], Yasunori Kohchi [a], Hitoshi Iikura [b], Yasuaki Matsubara [a], Kohsuke Asoh [a], Takeshi Murata [a], Masami Kohchi [a], Eisaku Mizuguchi [b], Shinji Tsujii [a], Kazuo Hattori [a], Takaaki Miura [a], Yasushi Yoshimura [a], Satoshi Aida [a], Masanori Miwa [a], Ryoichi Saitoh [b], Naoaki Murao [b], Hisafumi Okabe [a], Charles Belunis [c], Cheryl Janson [c], Christine Lukacs [c], Verena Schück [c], Nobuo Shimma [a]

[a] Kamakura Research Laboratories, Chugai Pharmaceutical Co., Ltd, 200 Kajiwara, Kamakura, Kanagawa 247-8530, Japan
[b] Fuji-Gotemba Research Laboratories, Chugai Pharmaceutical Co., Ltd, 1-135 Komakado, Gotemba, Shizuoka 412-8513, Japan
[c] Hoffmann-La Roche Inc., 340 Kingsland Street, Nutley, 07110 NJ, United States

ARTICLE INFO

Article history:
Received 17 October 2010
Revised 8 December 2010
Accepted 17 January 2011
Available online 21 January 2011

Keywords:
Allosteric MEK inhibitor
Orally available anticancer agent
[1,2]Oxazinan-3-one ring structure

ABSTRACT

The MAP kinase pathway is one of the most important pathways involved in cell proliferation and differentiation, and its components are promising targets for antitumor drugs. Design and synthesis of a novel MEK inhibitor, based on the 3D-structural information of the target enzyme, and then multidimensional optimization including metabolic stability, physicochemical properties and safety profiles were effectively performed and led to the identification of a clinical candidate for an orally available potent MEK inhibitor, CH4987655, possessing a unique 3-oxo-oxazinane ring structure at the 5-position of the benzamide core structure. CH4987655 exhibits slow dissociation from the MEK enzyme, remarkable in vivo antitumor efficacy both in mono- and combination therapy, desirable metabolic stability, and insignificant MEK inhibition in mouse brain, implying few CNS-related side effects in human. An excellent PK profile and clear target inhibition in PBMC were demonstrated in a healthy volunteer clinical study.

The mitogen-activated protein kinase (MAPK) pathway, including the Ras/Raf/MEK/ERK signaling cascade, is one of the most important pathways involved in cell proliferation and differentiation.[1] Aberrant activation of the MAPK pathway in tumor cells, such as K-Ras or B-Raf mutation, is frequently observed[2,3] and, therefore, the components of this pathway have promise as targets for antitumor drugs.[4,5]

Although several MEK inhibitors were clinically evaluated, clear clinical efficacy has not yet been observed. The development of CI-1040 (Pfizer Inc.), the first MEK inhibitor tested clinically, was terminated due to its insufficient efficacy and poor PK profile such as inter-patient variability, which may be a result of its low water solubility and metabolic instability, especially against hydrolysis of the hydroxamate moiety.[6] PD0325901 (Pfizer Inc.), the second MEK inhibitor, exhibited improved water solubility and stability against this metabolism. Oral administration to human of this drug, however, still afforded a certain amount of COOH metabolites. Furthermore, PD0325901 exhibited several side effects such as visual disturbance and syncope which implied the drug has an effect on the CNS.[7] These implied a demand for novel MEK inhibitors with superior efficacy and better physicochemical, metabolic and safety profiles. Thus, we initiated research to create a novel MEK inhibitor with the required profiles taking CI-1040 as a lead structure (Fig. 1).

Wabnitz et al. studied in vitro and in vivo metabolism of CI-1040 revealing that the hydroxamate moiety of CI-1040 is hydrolyzed by both cytochrome P450 enzymes and non-P450 amidase.[8] Although a preliminary attempt to replace the hydroxamate moiety with another functional group resulted in a reduction of MEK inhibitory activity (data not shown), we thought modification of another position might contribute to solving the problem of the hydrolysis by affecting the recognition by the metabolic

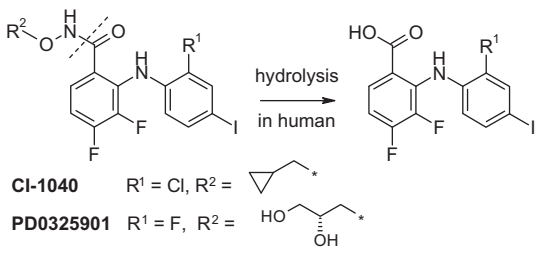

Figure 1. Structure of 1st and 2nd clinically tested MEK inhibitors and the major metabolic pathway.

* Corresponding author.
E-mail address: isshikiysa@chugai-pharm.co.jp (Y. Isshiki).

0960-894X/$ - see front matter © 2011 Elsevier Ltd. All rights reserved.
doi:10.1016/j.bmcl.2011.01.062

enzymes. From the point of maintenance of MEK inhibitory activity and synthetic feasibility, we focused on the modification of 5-position. The 5-substituted derivatives were synthesized via common intermediate **4** which was prepared starting with iodination of benzoic acid **1**[9] followed by vinylation[10] and nucleophilic aromatic substitution.[11] We discovered that the oxime ether derivatives

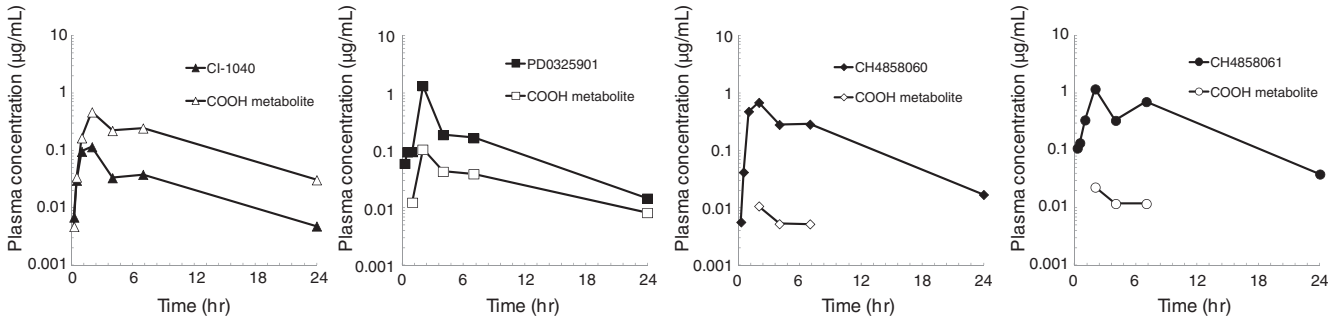

Figure 2. Time course of plasma concentration after single oral administration of CI-1040, PD0325901, CH4858060 and CH4858061 (2 mg/kg) in cynomolgus monkeys ($n = 2$). Values for drug concentration in plasma are given as the mean (μg/ml); ▲: intact CI-1040; △: COOH metabolite of CI-1040; ■: intact PD0325901; □: COOH metabolite of PD0325901; ♦: intact CH4858060 (**6**); ◇: COOH metabolite of CH4858060 (**6**); ●: intact CH4858061 (**7**); ○: COOH metabolite of CH4858061 (**7**).

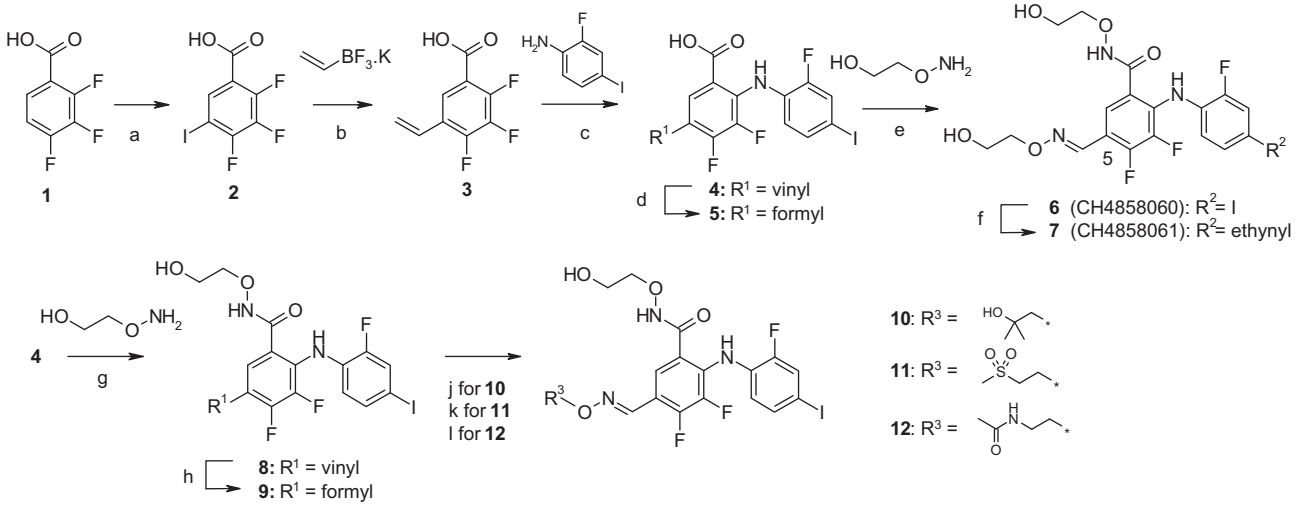

Scheme 1. Reagents and conditions: (a) I_2, MnO_2, Ac_2O, AcOH, H_2SO_4, 50 °C, 94%; (b) Pd(dppf)Cl_2, MeOH, reflux, 98%; (c) LiHMDS, THF, −78 °C–rt, 94%; (d) OsO_4 (cat.), $NaIO_4$, $NaHCO_3$, THF–H_2O, rt, 93%; (e) (i) WSC, HODhbt, THF, 91%; (f) (i)TMS–acetylene, $(PPh_3)_2PdCl_2$, CuI, THF, 79%; (ii) TBAF, THF, 74%; (g) WSC, HODhbt, DMF, 91%; (h) OsO_4 (cat.), $NaIO_4$, DMA, THF–H_2O, 56%; (j) 1-aminooxy-2-methyl-propan-2-ol, THF–CH_2Cl_2, 52%; (k) (i) *O*-(2-methylsulfanyl-ethyl)-hydroxylamine, THF–CH_2Cl_2, 90%; (ii) oxone, MeOH–H_2O, 63%; (l) (i) *O*-(2-amino-ethyl)-hydroxylamine, THF–CH_2Cl_2, 90%; (ii) *N*-methoxy-diacetamide, DMF, MeOH, 83%.

Table 1
Biological and physicochemical profiles of 5-substituted benzamide MEK inhibitors (part 1)

Core structure	Compound	R^1	R^2	In vitro IC_{50} (nM)			Solubility pH 6.5 (μM)	mLM $t_{1/2}$ (min)	hLM $t_{1/2}$ (min)	In vivo antitumor efficacy	
				MEK	HT-29 (CRC)	QG56 (NSCLC)				TGI(@MTD) in HT-29 p.o., qd × 14 days, $n = 6$ (%)	MTD (mg/kg)
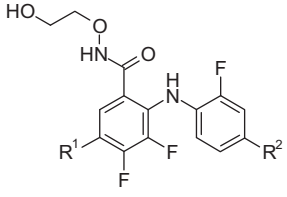	**6**	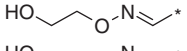	I	100	80	160	8.3	237	65	82	100
	7	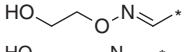	Ethynyl	235	150	160	415	135	80	82	>200
	10	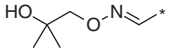	I	37	40	128	15	>360	>360	85	100
	11	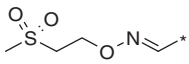	I	67	27	24	1	>360	90	98	>200
	12	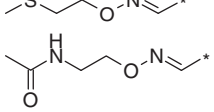	I	48	86	199	16	>360	>360	99	>200

CRC: colorectal cancer; NSCLC: non small cell lung cancer; mLM: mouse liver microsome; hLM: human liver microsome, TGI: tumor growth inhibition; MTD: maximum tolerable dose.
Detailed procedures for each assay listed in Tables 1–4 are described in the Supplementary data.

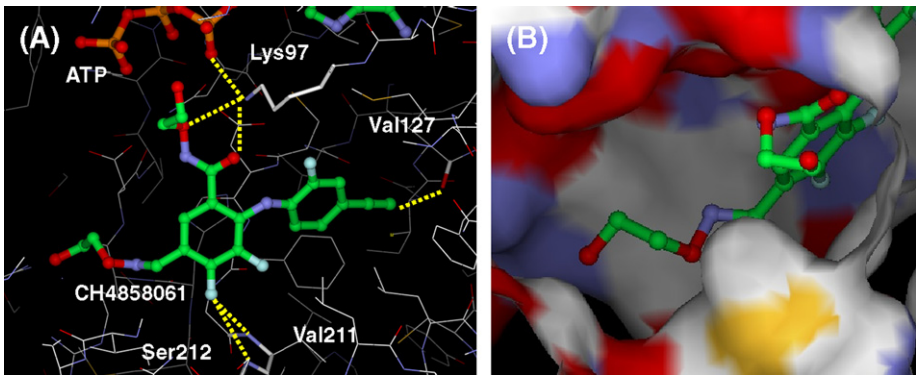

Figure 3. Ternary complex of CH4858061/MEK1/ATP (PDB code: 3OS3). (A) Overview; green: CH4858061; white: MEK1; orange: ATP; yellow dotted lines: intermolecular H-bondings and electrostatic interactions; (B) close-up of area around the oxime-ether side chain.

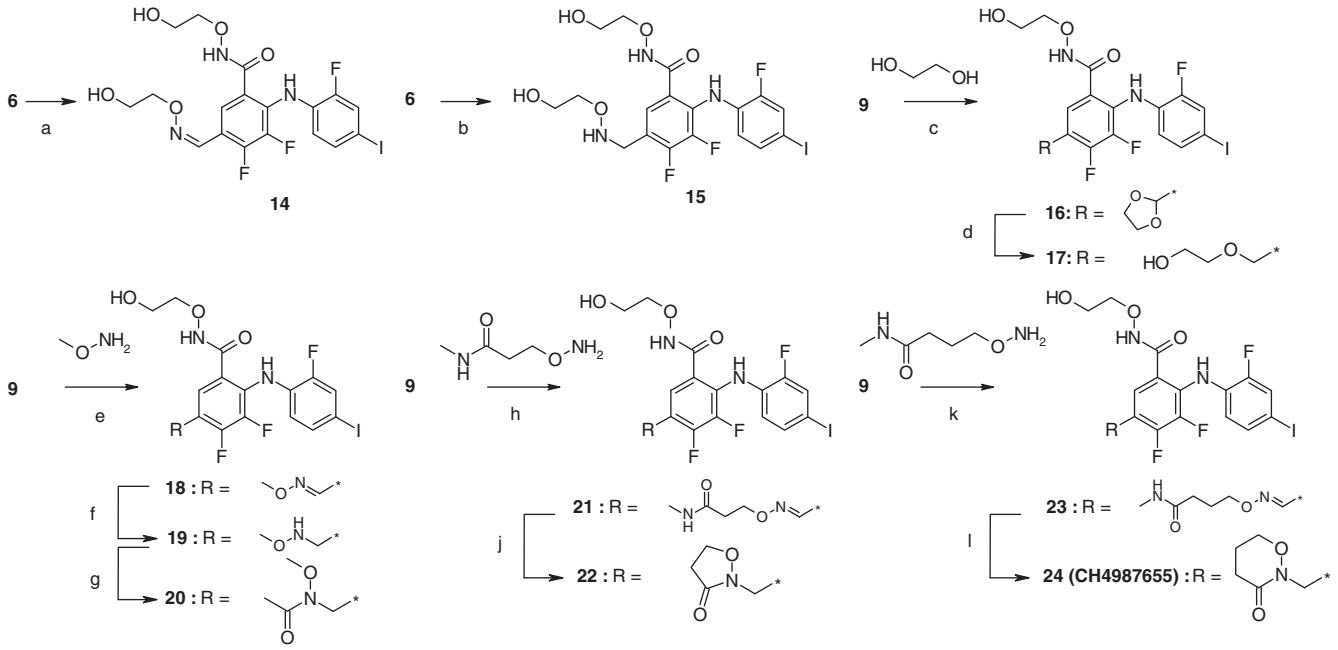

Scheme 2. Reagents and conditions: (a) $Cu(OTf)_2$, toluene, 60 °C, 81%; (b) $NaBH_3CN$, TFA, MeOH, rt, 46%; (c) TsOH (cat.), THF; (d) $NaBH_4$, TFA, THF, two steps 80%; (e) CH_2Cl_2, THF, 90%; (f) BH_3–pyridine, $CHCl_2COOH$, CH_2Cl_2, 93%; (g) CH_3COOH, EDC, HODhbt, Et_3N, CH_2Cl_2, 53%; (h) THF, MeOH, 80%; (j) BH_3–pyridine, $CHCl_2COOH$, CH_2Cl_2, rt, then 1,2-dichloroethane, 60 °C, 90%; (k) THF, MeOH, 80%; (l) BH_3–pyridine, $CHCl_2COOH$, CH_2Cl_2, rt, then 1,2-dichloroethane, 60 °C, 91%.

CH4858060 (**6**) and CH4858061 (**7**) showed significantly higher metabolic stability of the hydroxamate side chain compared to CI-1040 and PD03259091[12] after oral administration in monkeys as shown in Figure 2. Considering the fact that PD0325901 possessing hydrophilic 2,3-dihydroxypropyl group in its hydroxamate part still gives a certain amount of COOH metabolite in monkeys, it can be concluded that the oxime side chain newly introduced at 5-position dominantly contributes to the improvement of the metabolic stability against hydrolysis. This interesting remote-control nature of the metabolic stability encouraged us to further modify these oxime ether derivatives (Scheme 1).

Despite the excellent metabolic stability, CH4858060 (**6**) and CH4858061 (**7**), however, still had several drawbacks including insufficient water solubility, low human liver microsome stability, and weak enzyme inhibitory activity as well as antitumor activity both in vitro and in vivo. Chemical modification of a terminal part of the oxime side chain, such as introduction of alkyl (**10**), sulfonyl (**11**) or amide (**12**) moiety, did not lead to significant improvement (Table 1).

To overcome these problems, a 3D-structure of the ternary complex of **7**/ATP/MEK1 using X-ray crystallography was utilized. Compound **7** is located in almost the same position as other known allosteric MEK inhibitors and a hydrogen bond network among ATP, MEK1 and **7** is observed (Fig. 3A). The oxime ether side chain is located near the activation loop and a certain amount of space was noticed around it (Fig. 3B). It was thought that this space could be utilized for further modification of the lead compounds **6** and **7** to obtain higher activity and better physicochemical properties.

In order to fill up the space, we designed several types of derivatives, having different degrees of conformational flexibility and bulkiness of the C-5 substituents. The *Z*-oxime ether **14** was successfully prepared from the corresponding *E*-isomer **6** by treating with $Cu(OTf)_2$ under heating[13] and the alkoxylamines **15** and **19** were prepared by reducing the corresponding oxime-ethers. Reductive etheration of the benzaldehyde **9**, typically acetal-formation followed by reduction, afforded the benzylether **17**. The alkoxylamides **20** and **22** as derivatives possessing a branched or cyclic type of side chain were prepared by acylation of the

Table 2
Biological and physicochemical profiles of 5-substituted benzamide MEK inhibitors (part 2)

Core structure	Compound	R	In vitro IC_{50} (nM)			Solubility pH 6.5 (μM)	mLM $t_{1/2}$ (min)	hLM $t_{1/2}$ (min)	In vivo antitumor efficacy	
			MEK	HT-29 (CRC)	QG56 (NSCLC)				TGI (@MTD) in HT-29 p.o., qd × 14 days, n = 6 (%)	MTD (mg/kg)
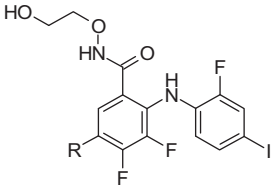	**6**	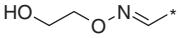	100	80	160	8.3	237	65	82	100
	14	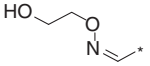	15	2.4	6	75	>360	>360	95	12.5
	17	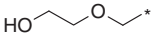	14	4.2	20	728	>360	>360	105	50
	15	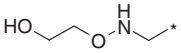	19	29	94	606	128	>360	93	100
	20	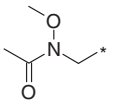	8.6	1.5	7.5	116	36	64	113	25
	22	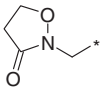	7.2	1.3	3.5	216	>360	>360	105	12.5

Table 3
Biological and physicochemical profiles of 5-substituted benzamide MEK inhibitors (part 3)

Core structure	Compound	R	In vitro IC_{50} (nM)			Solubility pH 6.5 (μM)	mLM $t_{1/2}$ (min)	hLM $t_{1/2}$ (min)
			MEK	HT-29 (CRC)	QG56 (NSCLC)			
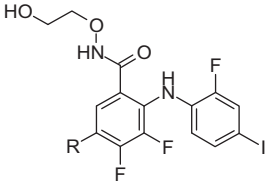	**22**	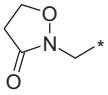	7.2	1.3	3.5	216	>360	>360
	25	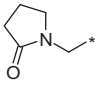	85	20	57	156	124	185
	26	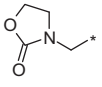	>250	560	3063	284	>360	>360
	27	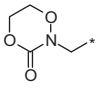	42	17	56	57	126	38

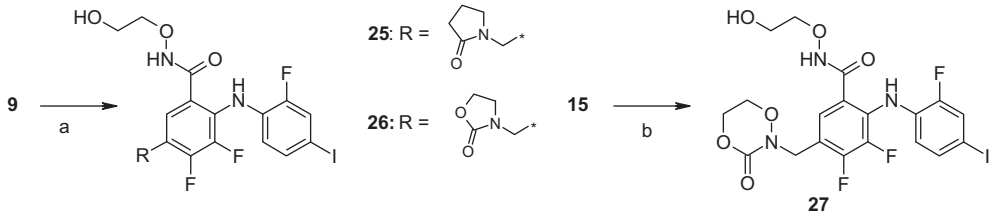

Scheme 3. Reagents and conditions: (a) preparation of **25**: 4-amino-butylic acid methylester hydrochloride, $NaBH_3CN$, MeOH, rt–reflux, 47%; preparation of **26**: (i) ethanolamine, CH_3COOH, $NaBH_3CN$, MeOH, 84%; (ii) *N*,*N*-disuccinimidyl carbonate, Et_3N, THF, CH_3CN, 42%; (b) *N*,*N*-disuccinimidyl carbonate, Et_3N, THF, CH_3CN, 12%.

corresponding alkoxylamine **19** or reduction of the oxime-ether **21** followed by simultaneous intra-molecular cyclization (Scheme 2).

The physicochemical and biological profiles of the representative derivatives are summarized in Table 2. As compared with *E*-oxime, the *Z*-oxime as well as the conformationally more flexible benzyl ether and alkoxy-amine derivatives showed higher water solubility, metabolic stability, and antitumor activity. The improved enzyme inhibitory activity of the *Z*-oxime **14** as compared with the *E*-oxime **6** suggested favorable conformation of the C-5 substituent that fits to the binding pocket. Interestingly, the cyclic

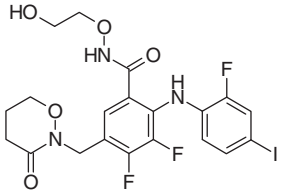

Figure 4. Structure of CH4987655.

Table 4
In vitro profile of CH4987655

Enzyme inhibition (IC_{50})		Tumor cell anti-proliferation (IC_{50})					Physicochemical property			In vitro safety profile		
MEK	Other 400 kinases	COLO205 (CRC, $Braf^{V600E}$)	HT29 (CRC, $Braf^{V600E}$)	QG56 (NSCLC, $Hras^{Q61L}$)	MIA PaCa-2 (Panc., $Kras^{G12C}$)	C32 (melanoma, $Braf^{V600E}$)	Solubility pH 6.5	Liver microsome stability (half life)		Drug–drug interaction	Genotoxicity	Cardio-toxicity
5.2 nM	<50% inhibition at 10 μM	0.86 nM	1.7 nM	9.5 nM	3.3 nM	8.4 nM	88 μM	Mouse >360 min	Human 116 min	CYP3A4 IC_{50} >100 μM	Ames MNT negative	hERG not significant

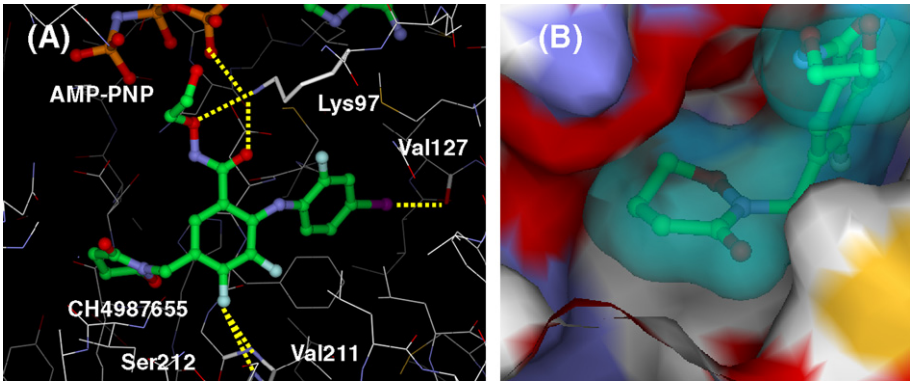

Figure 5. X-ray crystal structure of CH4987655/MEK1/AMP-PNP (PDB code: 3ORN). (A) Overview; green: CH4987655; white: MEK1; orange: AMP-PNP; yellow dotted lines: intermolecular H-bondings and electrostatic interactions; (B) close-up view around the newly introduced 3-oxo-oxazinan ring sub-structure.

derivative, isoxazolidinone **22**, exhibited the highest enzyme inhibitory activity and antitumor activity among these derivatives.

Evaluation of the cyclic system of **22** by modifying in particular the pattern of the heteroatom arrangement revealed that the O–N–C(=O)–C sub-structure was important for exhibiting the desired biological activity. For example, replacement of the ether oxygen by a methylene carbon dramatically reduced the MEK inhibitory activity (Table 3, Scheme 3).

Further optimization of **22** led us eventually to identify CH4987655 (**24**) (Scheme 2 and Fig. 4) as a clinical candidate having a unique 3-oxo-[1,2]oxazinan-2-ylmethyl group at the 5-position. The in vitro profiles of CH4987655 are summarized in Table 4. CH4987655 inhibits MEK with an IC_{50} of 5 nM, but did not inhibit the other 400 kinases at 10 μM. It showed strong in vitro anti-proliferative activity against a broad range of tumor cells without genotoxicity or hERG and CYP inhibition in vitro. Sufficient water solubility and in vitro metabolic stability was also observed.

X-ray crystal structure analysis of the ternary complex of CH4987655/MEK1/AMP-PNP showed H-bonding interaction of the hydroxamate oxygens with AMP-PNP through Lys97, and electrostatic interactions of the 4-fluorine with the backbone NHs of Val211 and Ser212, and 4′-iodine with backbone carbonyl of Val127 (Fig. 5A). Notably, the newly introduced [1,2]oxazinan-3-one ring structure occupies well the aforementioned open-space (Fig. 5B), surrounded by five amino acid residues, Gly210, His188, Arg189, Asn221 and Met219. In particular, the terminal aminocarbonyl moiety of Asn221 has moved greatly from its original position in the structure of CH4858061/MEK1/ATP to form a tighter space fitting the [1,2]oxazinan-3-one ring structure. Indeed, surface plasmon resonance (SPR) analysis revealed the higher affinity of CH4987655 for MEK1 compared with that of PD0325901 both in the absence and the presence of ATP, largely due to a slower dissociation (Table 5). Also, as reported previously for PD0325901,[14] the binding affinity of CH4987655 was significantly increased in the presence of ATP (Table 5), consistent with the intermolecular H-bonding network observed between CH4987655 and AMP-PNP in the MEK1 complex structure (Fig. 5A). The slower dissociation of CH4987655 from MEK1 could explain the observed superior pharmacodynamics of CH4987655 to PD0325901 in cynomolgus monkeys showing the longer pharmacodynamic duration with the lower IC_{50} value for pERK formation in PBMC (IC_{50} = 7.03 ng/mL for CH4987655 vs IC_{50} = 32.8 ng/mL for PD0325901).[15] The details of the interaction and the role of the newly introduced [1,2]oxazinan-3-one ring structure with MEK1 is now under investigation.

We examined the MEK inhibition status of CH4987655 in both tumor and brain in a HT-29 human colon cancer xenograft at the maximum tolerable dose (MTD), and compared it with that of PD0325901. Both CH4987655 and PD0325901 strongly inhibited pERK formation in tumor (Fig. 6A), and CH4987655 showed strong tumor regression at this dose (Fig. 7). Interestingly, a distinct difference was seen between the two drugs in the target inhibition in the brain. CH4987655 did not inhibit MEK in mouse brain at MTD, but PD0325901 did (Fig. 6B). This result can be explained by the very low distribution of CH4987655 to the brain as compared with the plasma concentration in a rat experiment (Fig. 6C).

CH4987655 demonstrated antitumor activity in a wide range of human cancer xenograft models. Strong tumor regression was observed in 70% of the models tested.[16] Examples of such strong antitumor efficacy with remarkable tumor regression are shown in

Table 5
Binding kinetics of MEK inhibitors to MEK1 in the presence or absence of ATP

Compound	−ATP		+ATP (50 μM)	
	K_D (nM)	K_{off} (/s)	K_D (nM)	K_{off} (/s)
CH4987655	8.7	8.00E-03	0.24	6.00E-05
PD0325901	31	1.70E-02	0.4	2.00E-04

The binding kinetics was measured by SPR analysis as described in the Supplementary data.

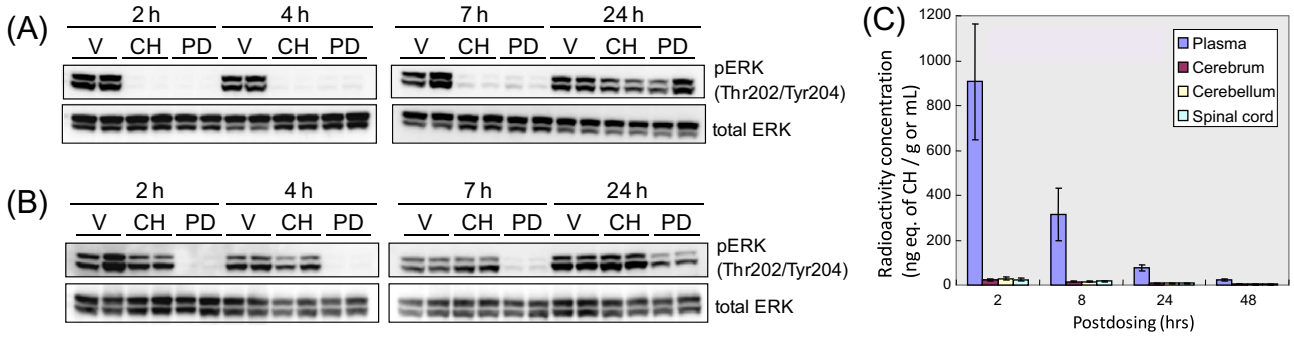

Figure 6. MEK inhibition status in HT-29 human colon cancer xenograft model after oral once-a-day treatment with CH4987655 (CH) at MTD (= 6.25 mg/kg), PD0325901 (PD) at MTD (25 mg/kg) and vehicle (V). (A) MEK inhibition status in tumor tissue; (B) MEK inhibition status in brain in mice; (C) distribution after oral administration of CH4987655 (1 mg/kg) into brain (cerebrum, cerebellum and spinal cord) as compared with into plasma in rat experiment.

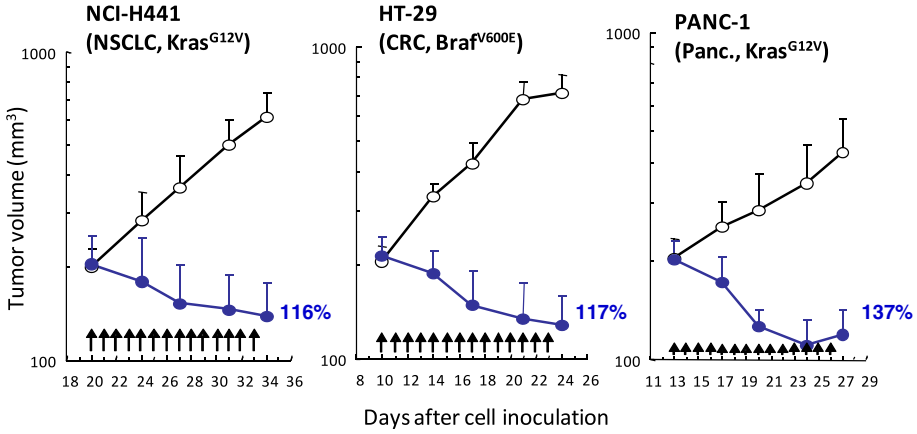

Figure 7. Antitumor effect of CH4987655 in human cancer xenograft models. Human tumor cell lines were subcutaneously transplanted into CAnN.Cg-Foxn1 nu/CrlCrlj mice. After confirmation of tumor implantation, the mice were randomly allocated into vehicle and drug-treated groups. CH4987655 was orally administered once-a-day at the maximum tolerated dose (MTD) for 14 days. Each group consisted of 6 mice. Values for tumor volume are given as the mean ± S.D.; ○: vehicle; ●: CH4987655. Percent tumor growth inhibition is shown to the right of each treatment group and values >100% indicate tumor regression.

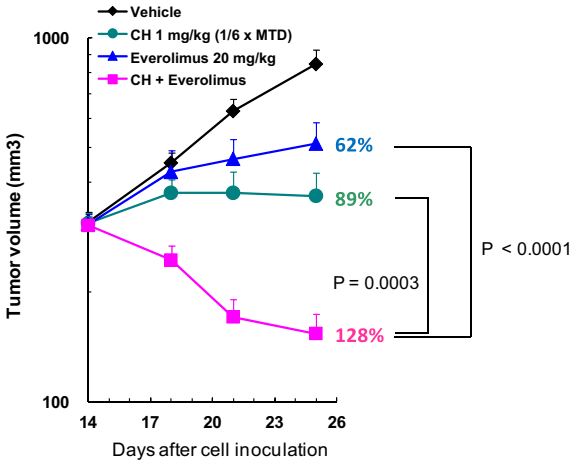

Figure 8. Antitumor effect of CH4987655 in combination with everolimus in HCT116(CRC, Kras^{G13D}) human cancer xenograft model. CH4987655 (1 mg/kg (1/6 MTD)) and everolimus (Sequoia Research Products Ltd) (20 mg/kg) were administered orally once daily for 11 days. Each group consisted of 5 mice (BALB-nu/nu (Crlj), male). Values for tumor volume are given as the mean ± S.D. ♦: vehicle; ▲: everolimus (20 mg/kg); ●: CH4987655 (1 mg/kg = 1/6 MTD); ■: CH4987655 (1 mg/kg) + everolimus (20 mg/kg); combo versus CH4987655: $P = 0.0003$; combo versus everolimus: $P < 0.0001$. Percent tumor growth inhibition is shown to the right of each treatment group and values >100% indicate tumor regression.

Figure 7. Furthermore, CH4987655 in combination with various antitumor agents enhanced the antitumor activity.[16] Concurrent oral treatment with CH4987655 (1 mg/kg = 1/6 MTD) and everolimus, the mTOR inhibitor, in HCT116 tumor-bearing mice showed greater antitumor activity compared to single-agent treatments showing clear tumor regression (Fig. 8).

As expected, oral CH4987655 showed higher metabolic stability than PD0325901 in cynomolgus monkeys: namely, the generation of COOH metabolites was much less in CH4987655. Exposures were dose–proportional and the AUC was about twice as high as that of PD0325901 (Fig. 9, Table 6).

This favorable PK profile was also confirmed by a phase 1 clinical trial in healthy volunteers. CH4987655 was rapidly absorbed after oral administration with a T_{max} of about 1 h and the disposition was biphasic with a terminal $t_{1/2}$ of about 25 h. Drug exposures were clearly dose–proportional within the tested dose, and very low inter-subject variability was observed. The effects of the target inhibition in PBMC were exposure-dependent and were greater than 80% at 4 mg. Good PK/PD correlation was observed.[17]

In summary, we discovered that the introduction of a unique oxime-ether side chain at 5-position of benzamide core structure dramatically improves the metabolic stability against hydrolysis of previously reported MEK inhibitors. Starting from such metabolically stable oxime-ethers **6** and **7** and utilizing the 3D-structural information, we identified a novel selective and potent MEK inhibitor, CH4987655 (**24**), possessing a unique 3-oxo-oxazinane ring

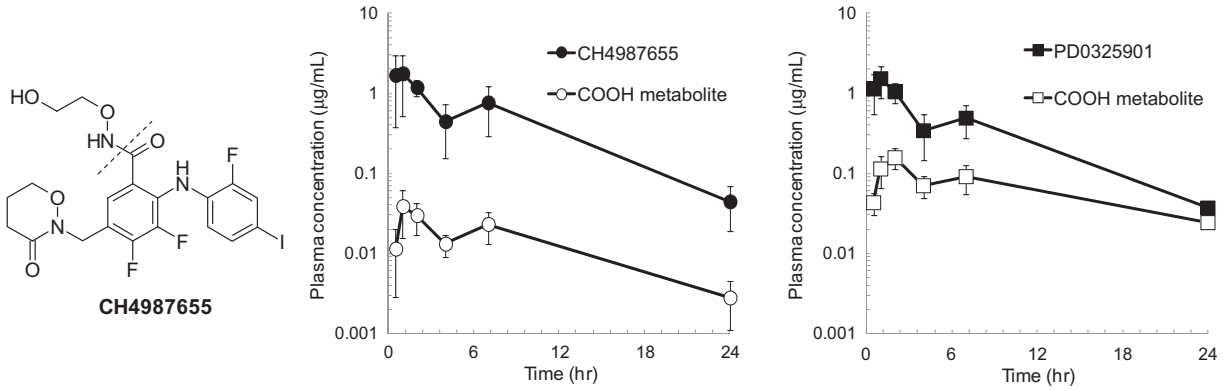

Figure 9. Time course of plasma concentration of CH4987655 and PD0325901 together with their COOH metabolites after oral single administration in cynomolgus monkeys ($n = 4$); Values for dug concentration in plasma are given as the mean ± S.D.; ●: intact CH4987655; ○: COOH metabolite of CH4987655; ■: intact PD0325901; □: COOH metabolite of PD0325901.

Table 6
PK parameters of CH4987655 and PD0325901 after oral single administration into cynomolgus monkeys

Compound	Dose (mg/kg)	T_{max} (h)	C_{max} (μg/ml)	AUC_{inf} (μg*h/ml)	$t_{1/2}$ (h)	MRT_{inf} (h)
CH4987655	1.5	1.3	0.4	2.2	6.6	8.4
	3	2.5	1	7.4	6	8.8
	6	1.5	2.1	10.4	5	7.3
PD0325901	6	1.1	1.7	7.9	5.5	7.3

structure at the 5-position. CH4987655 shows slow dissociation from MEK, high metabolic stability and remarkable in vivo antitumor efficacy with clear target inhibition in tumor but not in the brain. Combination therapy with the PI3K/Akt/mTOR pathway inhibitor significantly enhances the in vivo efficacy, exhibiting clear tumor regression. Favorable PK/PD profiles were observed in a healthy volunteer study. Taken together, we expect CH4987655 to be clinically effective with manageable toxicity. A phase 1 clinical study with solid tumor patients is currently in progress.

Acknowledgments

We are grateful to N. Oikawa, H. Koyano, T. Hayase, S. Takeda, K. Morikami, K. Yoshinari, Y. Itezono, N. Nakayama, H. Shirai, H. Shindo, T. Mitsui, T. Ueto, R. Takano, N. Inagaki, Y. Inagaki, Y. Tomii, E. Hashimoto, R. Watanabe, K. Hamada, Y. Tachibana, N. Ishii, A. Kubota, H. Suzuki, T. Shiga, H. Matsumoto, T. Tsuno, A. Kawashima and all people who contributed to this project.

Supplementary data

Supplementary data associated with this article can be found, in the online version, at doi:10.1016/j.bmcl.2011.01.062.

References and notes

1. Davis, R. J. *J. Biol. Chem.* **1993**, *268*, 14553.
2. Bos, J. L. *Cancer Res.* **1989**, *49*, 4682.
3. (a) Cohen, Y.; Xing, M.; Mambo, E.; Guo, Z.; Wu, G.; Trink, B.; Beller, U.; Westra, W. H.; Ladenson, P. W.; Sidransky, D. *J. Natl. Cancer Inst.* **2003**, *95*, 625; (b) Davies, H.; Bignell, G. R.; Cox, C.; Stephens, P.; Edkins, S.; Clegg, S.; Teague, J.; Woffendin, H.; Garnett, M. J.; Bottomley, W.; Davis, N.; Dicks, E.; Ewing, R.; Floyd, Y.; Gray, K.; Hall, S.; Hawes, R.; Hughes, J.; Kosmidou, V.; Menzies, A.; Mould, C.; Parker, A.; Stevens, C.; Watt, S.; Hooper, S.; Wilson, R.; Jayatilake, H.; Gusterson, B. A.; Cooper, C.; Shipley, J.; Hargrave, D.; Pritchard-Jones, K.; Maitland, N.; Chenevix-Trench, G.; Riggins, G. J.; Bigner, D. D.; Palmieri, G.; Cossu, A.; Flanagan, A.; Nicholson, A.; Ho, J. W. C.; Leung, S. Y.; Yuen, S. T.; Weber, B. L.; Seigler, H. F.; Darrow, T. L.; Paterson, H.; Marais, R.; Marshall, C. J.; Wooster, R.; Stratton, M. R.; Futreal1, P. A. *Nature* **2002**, *417*, 949; (c) Xu, X.; Quiros, R. M.; Gattuso, P.; Ain, K. B.; Prinz, R. A. *Cancer Res.* **2003**, *63*, 4561.
4. (a) Gollob, J. A.; Wilhelmb, S.; Carterb, C.; Kelleyb, S. L. *Semin. Oncol.* **2006**, *33*, 392; (b) McCubrey, J. A.; Milella, M.; Tafuri, A.; Martelli, A. M.; Lunghi, P.; Bonati, A.; Cervello, M.; Lee, J. T.; Steelman, L. S. *Curr. Opin. Investig. Drugs.* **2008**, *9*, 614; (c) Sebolt-Leopold, J. S.; Herrera, R. *Nat. Rev. Cancer* **2004**, *4*, 937; (d) Roberts, P. J.; Der, C. J. *Oncogene* **2007**, *26*, 3291.
5. (a) Sebolt-Leopold, J. S. *Curr. Pharm. Des.* **2004**, *10*, 1907; (b) McCubrey, J. A.; Steelman, L. S.; Abrams, S. L.; Chappell, W. H.; Russo, S.; Ove, R.; Milella, M.; Tafuri, A.; Lunghi, P.; Bonati, A.; Stivala, F.; Nicoletti, F.; Libra, M.; Martelli, A. M.; Montalto, G.; Cervello, M. *Expert Opin. Emerg. Drugs.* **2010**, *15*, 203.
6. (a) LoRusso, P. M.; Adjei, A. A.; Varterasian, M.; Gadgeel, S.; Reid, J.; Mitchell, D. Y.; Hanson, L.; DeLuca, P.; Bruzek, L.; Piens, J.; Asbury, P.; Becelaere, K. V.; Herrera, R.; Sebolt-Leopold, J.; Meyer, M. B. *J. Clin. Oncol.* **2005**, *23*, 5281; (b) Barrett, S. D.; Bridges, A. J.; Dudley, D. T.; Saltiel, A. R.; Fergus, J. H.; Flamme, C. M.; Delaney, A. M.; Kaufman, M.; LePage, S.; Leopold, W. R.; Przybranowski, S. A.; Sebolt-Leopold, J.; Becelaere, K. V.; Doherty, A. M.; Kennedy, R. M.; Marston, D., ; Howard, W. A., Jr.; Smith, Y.; Warmus, J. S.; Tecle, H. *Bioorg. Med. Chem. Lett.* **2008**, *18*, 6501.
7. (a) LoRusso, P.; Krishnamurthi, S.; Rinehart, J. R.; Nabell, L.; Croghan, G.; Varterasian, M.; Sadis, S. S.; Menon, S. S.; Leopold, J.; Meyer, M. B. *ASCO*, annual meeting , Abstract No. 3011, 2005.; (b) Haura, E. B.; Ricart, A. D.; Larson, T. G.; Stella, P. J.; Bazhenova, L.; Miller, V. A.; Cohen, R. B.; Eisenberg, P. D.; Selaru, P.; Wilner, K. D.; Gadgeel, S. M. *Clin. Cancer Res.* **2010**, *16*, 2450.
8. Wabnitz, P. A.; Mitchell, D.; Wabnitz, D. A. M. *Pharm. Res.* **2004**, *21*, 1670.
9. (a) Lulinski, P.; Skulski, L. *Bull. Chem. Soc. Jpn.* **1999**, *72*, 115; (b) Koyano, H.; Iikura, H.; Isshiki, Y.; Kohchi, Y. WO 2006109661.
10. Molander, G. A.; Rivero, M. R. *Org. Lett.* **2002**, *4*, 107.
11. (a) Chen, M. H. G.; Magano, J. WO 2000064856.; (b) Chen, M. H.; Beylin, V. G.; Iakovleva, E.; Kesten, S. J.; Magano, J.; Vrieze, D. *Synth. Commun.* **2002**, *32*, 411.
12. CI-1040 was prepared according to the description (Example 95) of WO99/01426. PD0325901 was prepared according to the description (Example 39) of WO02/06213.
13. As the first screening, several kinds of Brönsted and Lewis acid such as HCl, TsOH, PPTS, BF_3OEt_2, $Mg(OTf)_2$, $Cu(OTf)_2$ were attempted. Then metal screening, including Cu, Sc, Y, Hf, Zn, Sn as triflate, followed by solvent screening was performed to reveal $Cu(OTf)_2$/toluene as the best condition for the isomerization of the oxime ether **6**.
14. Smith, C. K.; Windsor, W. T. *Biochemistry* **2007**, *46*, 1358.
15. Yoshimura, Y.; Ishii, N.; Sakamoto, H.; Miura, T.; Isshiki, Y.; Ishikawa, Y.; Miwa, M.; Shimma, N.; Okabe, H.; Aoki, Y.; *AACR*, annual meeting, Abstract no. 2920, 2009.
16. Aida, S.; Yoshimura, Y.; Ishii, N.; Sakamoto, H.; Isshiki, Y.; Ishikawa, Y.; Miwa, M.; Shimma, N.; Okabe, H.; Aoki, Y.; *AACR*, annual meeting, Abstract no. 3701, 2009.
17. Lee, L.; Niu, H.; Rueger, R.; Igawa, Y.; Deutsch, J.; Ishii, N.; Mu, S.; Sakamoto, Y.; Busse-Reid, R.; Gimmi, C.; Goelzer, P.; Schepper, S. D.; Yoshimura, Y.; Barrett, J.; Ishikawa, Y.; Weissgerber, G.; Peck, R. *Clin. Cancer Res.* **2009**, *15*, 7368.